

miR-661 expression in SNAI1-induced epithelial to mesenchymal transition contributes to breast cancer cell invasion by targeting Nectin-1 and StarD10 messengers

Guillaume Vetter¹, Anne Saumet², Moes Michèle¹, Laurent Vallar³, Antony Le Béhec¹, Cristina Laurini¹, Michelle Sabbah⁴, Khalil Arar⁵, Charles Theillet², Charles-Henri Lecellier⁶, Evelyne Friederich^{1*}

¹ Cytoskeleton and Cell Plasticity Lab Université du Luxembourg, Life Sciences Research Unit-FSTC, L-1511 Luxembourg, LU

² IRCM, Institut de recherche en cancérologie de Montpellier INSERM : U896, Université Montpellier I, CRLCC Val d'Aurelle - Paul Lamarque, 208 rue des Apothicaires F-34298 Montpellier, FR

³ Centre de Recherche Publique- Santé Université du Luxembourg, Microarray Center 84, Val Fleuri L-1526 Luxembourg, LU

⁴ Centre de Recherche Saint-Antoine INSERM : U938, Université Paris VI - Pierre et Marie Curie, 75571 Paris, FR

⁵ Sigma-Aldrich Evry GENEPOLE, 5 rue Henri Desbruères 91000 Évry, FR

⁶ IGMM, Institut de génétique moléculaire de Montpellier CNRS : UMR5535, Université Montpellier II, 1919 Route de Mende 34293 Montpellier Cedex 5, FR

* Correspondence should be addressed to: Evelyne Friederich <evelyne.friederich@uni.lu >

Abstract

Epithelial to Mesenchymal Transition (EMT) is a key step towards metastasis. MCF7 breast cancer cells conditionally expressing the EMT master regulator SNAI1 were used to identify 8 early expressed miRNAs and their targets which may contribute to the EMT process. Potential targets of miRNAs were identified by matching lists of *in silico* predicted targets and of inversely expressed mRNAs. MiRNAs were ranked based on the number of predicted hits, highlighting miR-661, a miRNA with so far no reported role in EMT. MiR-661 was found required for efficient invasion of breast cancer cells by destabilizing two of its predicted mRNA targets, the cell-cell adhesion protein Nectin-1 and the lipid transferase StarD10, resulting, in turn, in the down-regulation of epithelial markers. Re-expression of Nectin-1 or StarD10 lacking the 3'-untranslated region counteracted SNAI1-induced invasion. Importantly, analysis of public transcriptomic data from a cohort of 295 well-characterized breast tumor specimen revealed that expression of StarD10 is highly associated with markers 8 of luminal subtypes while its loss negatively correlated with the EMT-related, basal-like subtype. Collectively, our *non-a priori* approach revealed a non-predicted link between SNAI1-triggered EMT and the down-regulation of Nectin-1 and StarD10 via the up-regulation of miR-661 which may contribute to the invasion of breast cancer cells and poor disease outcome.

MESH Keywords Breast Neoplasms ; genetics ; metabolism ; pathology ; Cell Adhesion Molecules ; genetics ; metabolism ; Cell Dedifferentiation ; drug effects ; genetics ; physiology ; Epithelial Cells ; metabolism ; physiology ; Female ; Gene Expression ; physiology ; Gene Expression Profiling ; Gene Expression Regulation, Neoplastic ; drug effects ; physiology ; Humans ; Mesenchymal Stem Cells ; metabolism ; physiology ; MicroRNAs ; genetics ; metabolism ; physiology ; Neoplasm Invasiveness ; Oligonucleotide Array Sequence Analysis ; Phosphoproteins ; genetics ; metabolism ; RNA, Messenger ; genetics ; metabolism ; RNA, Small Interfering ; pharmacology ; Transcription Factors ; genetics ; metabolism ; physiology ; Tumor Cells, Cultured ; Validation Studies as Topic

Author Keywords EMT ; miR-661 ; SNAI1 ; StarD10 ; Nectin-1 ; breast cancer cell invasion

Introduction

Epithelial to mesenchymal transition (EMT) is a fundamental, transient biological process implicated in gastrulation or neural crest cell migration during embryogenesis as well as in wound healing in adults. In addition, the complex EMT program is reactivated in carcinoma cells allowing them to dissociate from the primary tumour to invade the surrounding tissues and to disseminate to distant organ sites (Kalluri and Weinberg, 2009). During carcinoma progression, the hallmarks of EMT are the loss of intercellular junctions and the acquisition of a fibroblast-like motile and invasive phenotype, associated with the down-regulation of epithelial markers and the up-regulation of mesenchymal markers (reviewed in De Wever *et al.*, 2008 ; Sabbah *et al.*, 2008 ; Thiery and Sleeman, 2006). Signals triggering EMT elicit the expression of transcription regulators such as SNAI1 that orchestrate key events of this process and confer invasive behavior to epithelial cells from various origins (Cano *et al.*, 2000 ; De Craene *et al.*, 2005), SNAI1 induces EMT by directly binding to the promoter of genes encoding proteins, such as E-cadherin and claudins, and in consequence by repressing their transcription (reviewed in (Peinado *et al.*, 2007)). In addition to the profound alterations of the expression profiles of messengers RNA (mRNAs) encoding genes observed during EMT, recent findings show that microRNAs (miRNAs) which are ~22nt-long non-coding RNAs that coordinate gene expression at the post-transcriptional level, also contribute to this process (reviewed in (Cano and Nieto, 2008 ; Gregory *et al.*, 2008b)). MiRNAs are thought to inhibit virtually all steps of translation, from initiation to elongation, and also to cause the destabilisation of mRNAs through imperfect micro-homologies with the 3'UTR of the targeted mRNAs. (reviewed in (Kim *et al.*, 2009)). Because of the imperfect match between the sequences of miRNAs and their target mRNAs, public data-based *in silico* predictions yield

several hundreds of potential targets for a given miRNA, making the identification of miRNA targets challenging. Signals triggering EMT lead to the down-regulation of the miR-200 family which is required for the maintenance of the epithelial phenotype via the repression of ZEB-1, which has been described to be a negative regulator of E-cadherin (Gregory *et al.*, 2008a ; Korpál *et al.*, 2008 ; Park *et al.*, 2008). However, only few up-regulated miRNAs which contribute to EMT by destabilizing mRNAs have been identified so far. Among those, miRNA-9 was proposed to sensitize breast cancer cells to EMT-inducing signals arising from the tumour environment by suppressing E-cadherin expression ((Ma *et al.*)). The miRNA-155 which is regulated in normal mouse mammary gland cells by the TGF β triggered-Smad pathway, contributes to EMT by targeting RhoA (Kong *et al.*, 2008), whereas miR-29a contributes to this process via the suppression of tristetrapolin expression (Gebeshuber *et al.*, 2009). In addition, EMT is a highly dynamic process, making the analysis of early modifications of the repertoire of miRNAs and of their mRNAs targets challenging.

Here, we performed a systematic, time-resolved screening to identify miRNAs which are differentially expressed at early time points of SNAI1-induced EMT in human breast cancer MCF7 cells previously characterized (Vetter *et al.*, 2009). By a non-*a priori* approach which combined large scale transcriptomic and *in silico* data analysis, we were able to identify miR-661 as a novel EMT-associated miRNA and Nectin-1 and StarD10 as two of its targets. In addition, we showed for the first time that miR-661 as well as its targets contributed to EMT-associated breast carcinoma cell invasion. Importantly, in contrast to Nectin-1, the expression of StarD10 positively associated with markers of luminal subtypes of breast carcinomas while it negatively correlated with markers of the EMT-related basal-like phenotype.

Results

Time-resolved transcriptomic analysis of early expressed miRNAs during EMT in MCF7-SNAI1 cells

To identify miRNAs which are differentially expressed during EMT, we used MCF7-tet off cells that conditionally express human SNAI1 under the control of tetracycline (Vetter *et al.*, 2009). These cells, termed MCF7-SNAI1, which express SNAI1 as early as 2 h after induction, allow to study transcriptional events during EMT in a time-resolved manner, in parallel to phenotypic modifications (Vetter *et al.*, 2009). In agreement with previously reported morphological modifications of these cells, epifluorescence microscopy analysis revealed that typical EMT-linked changes such as the reorganization of the actin cytoskeleton and the down-regulation of cytokeratin-18 and E-cadherin, started 12 h after induction (Figure 1A and (Vetter *et al.*, 2009)). Concomitant to phenotypic changes, SNAI1 expression readily increased the migration and invasion capacity of MCF7 cells in transwell assays when compared with non-induced cells (Figure 1B and 1C , respectively). A time series of microarray-based miRNA expression profiling experiments was performed between 4 h and 96 h after SNAI1 induction. Interestingly, down-regulation of miR-200 family members (miR-200a, miR-200b and miR-429) which are known to negatively regulate EMT (Cano and Nieto, 2008) was observed in our cell model, 12 h after SNAI1-induction (Figure 1D), an observation which was confirmed by real-time PCR (Supplemental data 1A). To identify miRNAs which may orchestrate the cascade of events leading to EMT via the down-regulation of mRNAs, we decided to focus on early up-regulated miRNAs (at a time point preceding 12 h after SNAI1 induction) whose expression constantly increased after SNAI1-7 induction. 26 miRNAs corresponding to these criteria were identified (Figure 1E). To rank these miRNAs for their potential impact on mRNAs in SNAI1-induced MCF7 cells, we assumed that miRNAs which are central to the regulation of epithelial homeostasis and EMT may target several mRNAs. To narrow-down the huge number (up to 500 hits) of *in silico* predicted target genes of the 26 early up-regulated miRNAs to a list of high confidence target candidates, we took advantage of the fact that miRNAs destabilize many of their targets (Baek *et al.*, 2008 ; Saumet *et al.*, 2009). Making use of available time-resolved mRNA profiling data obtained with MCF7-SNAI1 cells (Vetter *et al.*, 2009), we first established a list of mRNAs the expression of which was inversely correlated with that of the up-regulated miRNAs following SNAI1-induction. Second, we matched this list with the one of the *in silico* predicted targets using miRBase Targets software (<http://microrna.sanger.ac.uk/>) of each of the 26 miRNAs. The number of targets predicted by this approach for an individual miRNAs ranged from 1 to 28. MiR-661 was predicted to target most of the down-regulated mRNAs (28 hits, Figure 1E). In support of the biological relevance of these findings, only a few up-regulated messengers were predicted to be targeted by miR-661 (Figure 1E). Early up-regulation of miR-661 was observed at 4 h and its expression reached the highest level at 96 h after SNAI1 induction, as confirmed by RT-qPCR (Figure 1F). This strong predictive participation of miR-661 in the regulation of mRNA translation during the early phase of EMT prompted us to further investigate its function in this process.

Inhibition of miR-661 decreased migration and invasion capacities of breast cancer cells

To assess the contribution of endogenous miR-661 to EMT-associated events, we inhibited its action by treating MCF7-SNAI1 cells with miR-661-specific antisense Locked Nucleic Acids (LNA-661) oligonucleotides (Lecellier *et al.*, 2005), prior to the induction of SNAI1. Cy3-coupled LNAs were used to determine the transfection efficiency which was about 70% of the total cell population (data not shown). Transfection of LNA-661 did not cause detectable changes of the cell phenotype under the present experimental conditions (data not shown), but reduced the migration and invasion capacities of induced MCF7-SNAI1 cells by 40% and 35%, respectively, when compared to induced cells transfected with a scrambled LNA (LNA-sc), used here as a negative control (Figure 2A). As shown in the Supplemental data 1B , these effects were not due to a decrease of cell proliferation.

Next, we decided to evaluate whether the reduction of the cell motility mediated by inhibition of miR-661 correlated with gene regulatory events participating to SNAI1-induced EMT and invasion in MCF7 cells. Thus, we assessed by real-time PCR the expression of EMT markers and/or of genes with an expected impact on invasion in induced-MCF7-SNAI1 cells treated with LNA-661 or LNA-sc. We observed a significant reduction of the repression of epithelial markers including Cytokeratin-18, Claudin-3, E-cadherin and Beta-catenin (Figure 2B). However, *in silico* predictions had not revealed binding sites for miR-661 in the 3'-UTR of these genes (see the approach described above) suggesting that their down-regulation by miR-661 is indirect, implicating so far non-identified direct targets of this miRNA. Conversely, LNA-661 did not affect the up-regulation of mesenchymal markers (including ZEB1, SNAI2 and SPARC) induced by SNAI1 expression (data not shown).

To determine whether the up-regulation of miR-661 was more generally correlated with the invasive behavior of breast carcinoma cells, we analysed its expression in non-invasive, (HMEC, MCF10F), weakly invasive breast cancer cells (T47D, MCF7) or in highly invasive cell lines (MDA-435 and MDA-231). Consistent with its role in breast cancer cell invasion, miR-661 was highly expressed in mesenchyme-like, invasive cells compared to non-invasive HMECs (Figure 2C), an expression pattern which correlated with the one of SNAI1 (Supplemental data 1C). Furthermore, similar to induced MCF7-SNAI1 cells, LNA-661 transfection decreased the migration and invasion capacity of highly invasive MDA-435 cells by 37% and 42% respectively, compared with scrambled LNA transfected control cells (Figure 2D). No effect was observed on cell phenotype or proliferation (data not shown and Supplemental data 1D).

Taken together, our observations suggest that early up-regulation of miR-661 may play a key role in the down-regulation of epithelial messengers which are required for EMT-associated invasion of carcinoma cells.

Biological validation and characterisation of predicted miR-661 targets

Next, we analyzed the effect of ectopically expressed miR-661 on the stability of its predicted target messengers (Figure 1E) in transfected MCF7 cells. E-cadherin mRNA, which is directly down-regulated by SNAI1 (Batlle *et al.*, 2000), but which is not a predicted target of miR-661, was used as a negative control. As monitored by RT-qPCR, ectopic expression of miR-661 (Supplemental data 1E) did neither change the level of E-cadherin mRNA nor that of 26 of its potential targets (Figures 3A and 3B, representative mRNAs are shown). In contrast, Nectin-1 and StarD10 decreased at both mRNA and protein levels, as compared to control cells transfected with the empty pSuper vector (Figures 3B and 3C). As shown in the Figure 3D, the expression of Nectin-1 and StarD10 negatively correlated with that of miR-661 (Figure 1F) in a time course experiment in SNAI1-induced MCF7 cells. The Nectin-1 mRNA decreased between 8 h and 12 h (Figure 3D top) whereas StarD10 mRNA decreased between 12 h and 24 h after SNAI1-induction (Figure 3D bottom). We performed an immunofluorescence analysis of Nectin-1 and StarD10 in non-induced and induced MCF7-SNAI1 cells. While Nectin-1 localized, as expected, to cell-cell contacts and codistributed with E-cadherin (reviewed in (Takai *et al.*, 2008)) in non-induced MCF7-SNAI1 cells (Figure 4A), StarD10 exhibited an as yet undescribed localisation to the plasma membrane, and partially co-distributed with the adherens or tight junctional markers E-cadherin and ZO-1, respectively (Figures 4B and 4C, respectively). As expected, no immunofluorescence signals were detected for Nectin-1 and StarD10 in induced MCF7-SNAI1 cells (Figures 4D and 4E, respectively).

To corroborate the specificity of the regulation of Nectin-1 and StarD10 by miR-661 we treated induced MCF7-SNAI1 cells with an anti-miR-661 LNA which was meant to protect *bona fide* endogenous mRNA targets of this miRNA from its destabilizing action. In contrast to other predicted candidates (NQO2, FLII, RNPEL1, and CACNAH1) or to the E-cadherin control, which were down-regulated in SNAI1-expressing MCF7 cells, LNA-661 specifically inhibited the down-regulation of the Nectin-1 and StarD10 messengers (Figure 5A). Immunoblot analysis of cell extracts confirmed the stabilization of Nectin-1 and StarD10 at the protein level, after LNA-661 transfection (Figure 5B; compared lanes 3 to lanes 4). To confirm that the 3'UTRs of Nectin-1 and StarD10 messengers which contains the miR-661 binding site are targeted by miR-661, we cloned the 3'UTR of both candidates downstream of *renilla* luciferase reporter gene (psiCHECK2-3'UTRnectin-1 and psiCHECK2-3'UTRStarD10). As expected, Renilla activity decreased when the two fusion constructs were transfected into induced MCF7-SNAI1 cells expressing the miR-661, compared with non-induced MCF7-SNAI1 cells (data not shown). However, the cotransfection with LNA-661 but not with LNA-sc markedly reduced the decrease of Renilla activity in induced MCF7-SNAI1 cells (Figure 5C). Collectively, these results show that Nectin-1 and StarD10 mRNAs are sensitive to miR-661 in epithelial cells undergoing EMT, suggesting their implication in this process.

Nectin-1 and StarD10 participate to SNAI1-elicited EMT and invasion

Consistent with the observations made in MCF7-SNAI1 cells, Nectin-1 and StarD10 messengers were found expressed in the poorly invasive epithelial cells (MCF7 and T47D) which express low levels of miR-661 (Figure 2C), while an inverse expression pattern was observed in the highly invasive fibroblastic-like breast carcinoma cells (MDA-231 and MDA-435) (Figures 6A and 6B, respectively). Since miR-661 expression contributed to the down-regulation of epithelial marker genes in EMT driven by SNAI1 (Figure 2B), we wanted to determine whether these regulations were mediated by its targets nectin-1 and StarD10 in epithelial breast cancer cell lines. We performed an RNAi directed against these two genes in the T47D, MCF7 breast epithelial cell lines and evaluated by real-time PCR the expression of epithelial and mesenchymal markers. The silencing of both genes in the two cell lines was confirmed by real-time PCR (Supplemental data 2A). Importantly, consistent with the effects of miR-661 (Figure 2B), the suppression of its two target genes

significantly reduced the expression of epithelial markers Cytokeratin-18, E-cadherin, beta-catenin, and claudin-3 in both cell lines, whereas the expression of mesenchymal markers did not change (Figure 6C and data not shown, respectively). This finding suggested that Nectin-1 and StarD10 may be part of the same or of converging regulatory pathways which control the expression of these epithelial genes.

Next, to investigate the relative contribution of Nectin-1 and StarD10 to EMT-related invasion, these proteins were ectopically expressed in induced MCF7-SNAI1 cells to evaluate whether they may overcome the invasion-promoting effect of miR-661. Cells were transfected with Nectin-1 or StarD10 GFP fusion variants lacking the 3'-untranslated region. The expression of the corresponding mRNAs was quantified by real-time PCR (Supplemental data 2B). GFP-fusion proteins exhibited the same sub-cellular localization (data not shown) than the endogenous proteins. Invasion assays showed that forced expression of GFP-Nectin-1 and GFP-StarD10 decreased by 31 % and 18% respectively cell invasion in induced MCF7-SNAI1 cells as compared to the GFP control (Figure 6D).

Altogether, these results suggest that the repression of Nectin-1 and StarD10 via miR-661 contributes to efficient SNAI1-mediated cell invasion triggered by the EMT program and that both proteins may act in concert with other regulators to maintain the epithelial cell state.

StarD10 is a novel molecular marker of the EMT-associated basal-like breast tumor subtype

Our results highlight for the first time that the loss of Nectin-1 and StarD10 in breast carcinoma cells is associated with EMT which is a key step towards metastasis. To evaluate the potential of these proteins in molecular breast tumor subtype classification, we performed a multiclass ANOVA statistical analysis with a previously characterized cohort of 295 breast cancer specimen, classified into cancer subtypes based on gene expression profiles and disease outcome (Fan *et al.* , 2006 ; van de Vijver *et al.* , 2002). StarD10 showed a strong statistical association with breast cancer subtypes (P-value = 4.910E-26), suggesting that StarD10 expression correlated also with the disease outcome in these 295 patients (Figure 7). In contrast to the cell-cell adhesion molecule Nectin-1 for which no association was determined (data not shown) the StarD10 was expressed in Luminal A, B (LA and LB) and Her2+ (HR) tumor subtypes (Figure 7), whereas its expression was low in the basal-like subtype (BL) which has been reported to exhibit molecular characteristics of EMT (Sarrío *et al.* , 2008). To corroborate this finding, we determined whether the expression of StarD10 correlated with known molecular markers of the basal-like and luminal subtypes in the cohort of 295 breast cancer tumors (Fan *et al.* , 2006 ; van de Vijver *et al.* , 2002). Whereas the expression of the luminal molecular markers FOXA1, GATA3, KRT18 and KRT8 (reviewed in (Lacroix, 2006)) in our dataset exhibited a positive Pearson correlation with that of StarD10, expression of the basal-like markers KRT5, KRT14 and FOXC1 (reviewed in (Lacroix, 2006)) showed a negative correlation (Table 1). Taken together, these findings suggest that the expression of StarD10 allows to discriminate the basal-like subtype from other major cancer subtypes. Thus, the loss of StarD10 may be a novel molecular marker for the EMT-associated basal-like breast cancer subtype.

Discussion

Malignant cancer cells are known to reactivate a program leading to EMT which also plays a crucial role during physiological process such as embryonic development and wound healing in adults. The MCF7-SNAI1 based-profiling assay that was previously established (Vetter *et al.* , 2009) allowed us to associate a specific miRNA expression signature with early events and to identify novel up-regulated miRNAs. We demonstrated that, when combined with *in silico* predictions, the time-resolved inverse expression correlation approach we developed was very powerful to identify high confidence target candidates of the miRNAs which were differentially expressed during SNAI1-mediated EMT. Our results highlighted miR-661, a miRNA has no reported function in EMT so far, as an important player in the regulatory 0 network leading to cancer cell invasion. In addition, among the predicted targets of miR-661, we experimentally confirmed an interaction between miR-661 and StarD10 or Nectin-1, and showed that they contribute to EMT-elicited cell invasion via the repression of epithelial genes. Importantly, our study revealed for the first time that the loss of StarD10 may be a highly relevant marker for the basal-like, EMT-associated, molecular subtype of breast cancer. Collectively, these findings design a new way for the dissection of regulatory 6 networks contributing to SNAI1-triggered EMT.

Our findings emphasize the importance of miRNA-triggered down-regulation of cell-cell contact proteins during EMT and cancer cell invasion and are in concordance with those recently made by (Ma *et al.*) which underline the role of the miR-9 in targeting the E-cadherin during epithelial cell transformation. Indeed, our data suggest that miR-661, via the de-stabilization of its two targets Nectin-1 and StarD10, may contribute to the efficient down-regulation of genes which contribute to the establishment and maintenance of the epithelial phenotype. Indeed, miR-661 targeted Nectin-1 which is known to participate in epithelial cell polarity and migration via the regulation of cell-cell junctions and cytoskeleton organization (reviewed in (Sakisaka *et al.* , 2007)). As supported by previous data, the repression of Nectin-1 by miR-661 may contribute to the disassembly of cell-cell contacts, an early step of EMT. In addition, as supported by the fact that its silencing affected the expression of epithelial genes, it is likely that Nectin-1, in addition to its structural role, also contributes to gene regulation. Such a dual function has been described for other cell junction proteins, including E-cadherin (Onder *et al.* , 2008).

While endogenous expression of miR-661 was required for efficient cell invasion, its ectopic over-expression did not significantly modify the migratory or invasive behavior of MCF7 cells (data not shown) suggesting that miR-661 may act in synergy with other factors.

Consistently, silencing of both of its targets in two independent breast cancer epithelial cell lines (T47D, MCF7) affected negatively the messenger level of epithelial genes (Figure 2B and Figure 6C, respectively) but was not sufficient to drive an EMT (data not shown). The contribution of other miRNAs during the EMT process is sustained by the observation that miR-200 family members were down-regulated in SNAI1-expressing MCF7 cells. Interestingly, in contrast to miR-661, members of the miR-200 family were down-regulated at later time points, suggesting that in the cascade of molecular events leading to EMT, regulation of miR-661 may precede that of the miR-200 family. The miR-200 family inhibits EMT and cancer cell migration by targeting the ZEB1 and ZEB2 oncogenes which directly repress transcription of the E-cadherin gene, a key cell-cell adhesion molecule of adherens junctions (Gregory *et al.*, 2008a; Hurteau *et al.*, 2007; Korpál *et al.*, 2008). Conversely to the miR-200 family which indirectly regulates E-cadherin, our results support a direct regulation of the Nectin-1 messenger by miR-661. Furthermore, re-expression of Nectin-1 could overcome the invasion promoting effect of miR-661. However, miR-661-mediated decrease of Nectin-1 was not sufficient to trigger dissociation of cell-cell contacts and an EMT phenotype (data not shown). This may be explained in part by the functional redundancy of Nectin isoforms that are expressed in MCF7 cells (Supplemental data 2C). In line, knock-out of Nectin-1 in a mouse model yielded only a moderate phenotype (reviewed in (Takai *et al.*, 2008)), whereas expression of a dominant negative variant of Nectin-1 perturbed epithelial cell morphogenesis (Brakeman *et al.*, 2009). In addition, our findings support the view that SNAI1 as well as miR-661 and miR-200 family members which are directly or indirectly regulated by SNAI1, may act in concert to control epithelial cell plasticity by targeting components of cell-cell junctions.

MiR-661 has been recently reported to be directly up-regulated by the transcription factor c/EBPalpha and to target metastatic tumor antigen 1 (MTA-1) in an ectopic forced expression assay (Reddy *et al.*, 2009). We neither detected a differential expression of c/EBP alpha nor of MTA-1 in our EMT model (data not shown). These findings support the view that several transcription factors may regulate a specific miRNA which may have distinct targets and effects depending on the cellular state and of its expression level. In line, miR-29a was recently shown to act either as an oncogene or as a tumour-suppressor depending on the cellular context (Gebeshuber *et al.*, 2009).

StarD10, the second direct target of miR-661, has been previously identified as a breast carcinoma-associated protein (Olayioye *et al.*, 2005). Conversely to Nectin-1, little information is available on the function of StarD10 in epithelial cells. StarD10 was proposed to mediate lipid transfer between intracellular membranes, a process which may contribute to processes such as epithelial cell polarity and signaling (Olayioye *et al.*, 2005). In support of such a role, we observed that StarD10 mainly localized to the plasma membrane and co-localized with junction markers. Whether StarD10 contributes directly or indirectly to the assembly and maintenance of cell-cell contacts requires further investigations. Interestingly, silencing of StarD10 resulted in the down-regulation of the same epithelial genes as observed for Nectin-1 silencing, suggesting coordinate action.

While over-expression of StarD10 has been shown to correlate with that of c-erbB and cancer cell transformation, a recent clinical study has reported the correlation of the loss of StarD10 with a group of poor prognosis breast cancers (Murphy *et al.*, 2009). Our findings which show one of the molecular mechanisms of regulation of the StarD10 expression during EMT, may reconcile these apparently controversial results. Consistent with previous data (Olayioye *et al.*, 2004), we found that StarD10 protein is over-expressed in weakly invasive breast cancer cells such as MCF7 or T47D cells when compared to normal breast epithelial cells (Figure 6B). Conversely, StarD10 was strongly repressed during SNAI1-induced EMT suggesting that transient, miR-661 mediated down-regulation of StarD10 may occur during cancer progression. In agreement, expression of StarD10 negatively correlated with markers of the basal-like subtype which bears mesenchymal molecular features and phenotype (Sarrío *et al.*, 2008) in a cohort of breast cancer tumors (Table 1). Thus, one might speculate that the expression of StarD10 may be correlated with the differentiation status of breast epithelial cells. In line with this hypothesis, it has been reported that StarD10 expression increased during terminal differentiation of breast epithelial cells reaching its maximum at pregnancy and lactation (Olayioye *et al.*, 2004). It can, however, not be excluded that additional factors including transcription factors and other early-up-regulated miRNAs may also contribute to its robust down-regulation in the basal-like breast cancer subtype.

Collectively, our results point to an important role for miR-661 in cancer cell invasion, a process to which its targets Nectin-1 and StarD10 may contribute. In the future, the loss of StarD10 expression may be used as a novel marker of basal-like tumors which exhibit mesenchymal features. Our study also paves the way to further explore the dynamic regulatory networks underlying SNAI1-mediated EMT.

Material and Methods

Cell culture

The generation of stable MCF7-SNAI1 cells has been described before (Vetter *et al.*, 2009). T47D, MDA-231 and MDA-435 cells were cultured in DMEM supplemented with 10 % FBS, 2 mM L-glutamine, 100 U/ml penicillin and 100 µg/ml streptomycin. Total RNA from Human Mammary Epithelial Cells (HMEC) and MCF10F cells was a gift from Michele Sabbah's laboratory.

Invasion and motility assays

For invasion and motility assays, 5.0×10^5 cells were cultured for 24 h in Matrigel-coated or uncoated Boyden chambers (8 μ m pores; BD Biosciences). 24 h after plating, cells were transfected with Lipofectamine 2000 (Invitrogen) (100 pmol siRNA (Qiagen), 100 nM LNA (Sigma-Proligo), or 4 μ g pSuper vector (OligoEngine)). MCF7-SNAI1 cell induction was realized 4 h after transfection. Cell migration/invasion to the lower side of the filter was evaluated with the MTT colorimetric assay (Sigma-Aldrich).

Cell proliferation analysis

Transfected cells were detached 24 h after transfection and plated in 12-well plates at a density of 5.10^4 cells/well in DMEM containing 10% FBS. Cell proliferation was evaluated using the MTT assay during 4 days.

Quantitative RT-PCR detection of mRNAs and miRNAs

Total RNA extraction from cells was performed with the Trizol reagent (Invitrogen). Reverse Transcription was realized with random primer (Invitrogen) for mRNA or with specific stem-loop oligonucleotides for miRNA detection as described recently in (Saumet *et al.*, 2009). Oligonucleotides used for miRNA and mRNA detection are detailed in Supplemental method 1.

Constructs

The precursor of the miR-661 was amplified by PCR from human genomic DNA using gaagatctCCTCCACAGAGCAGGG as sense and cccaagctGGTGCTCTTGAAAGGC as antisense oligonucleotide. The resulting amplicon was cloned into the *Bgl* II/*Hin* dIII restricted pSuper-retro vector (OligoEngine). For the ectopic expression of Nectin-1 and StarD10, cDNAs were extracted from the hORFeome V5.1 (<http://horfdb.dfci.harvard.edu/>) and cloned into the pL30-GFP3X vector using the Gateway technology (Invitrogen).

Immunofluorescence and immunoblotting

For immunofluorescent staining, cells grown to 60–80% confluency were processed as previously described (Vetter *et al.*, 2009), prior to the addition of primary and fluorescently-labeled anti-IgG secondary antibodies. Visualization of E-cadherin was performed by labeling with mouse-anti-E-cadherin (BD Transduction Labs), SNAI1 with Goat-anti-SNAI1 (Santa Cruz), Cytokeratin-18 with mouse-anti-Cytokeratin-18 (Santa Cruz), Nectin-1 (PVRL1) with rabbit-anti-Nectin-1 (Santa Cruz), StarD10 with goat-anti-StarD10 (Santa Cruz), respectively. Actin cytoskeleton and nuclei were stained with phalloidin-350 (Invitrogen), and DAPI (Sigma), respectively. Fluorescence imaging was realized by confocal microscopy (LSM510, Zeiss), and phase contrast imaging using an inverted microscope (Leica). Immunoblot analyses were carried out using the same primary antibodies that used for immunofluorescence assays. Detection of gapdh using the anti-mouse-gapdh (Sigma-Aldrich) was performed in order to estimate the protein amount loaded in each well. Secondary antibodies against mouse, goat, rabbit coupled with HRP (Promega) were used for the immunodetection.

DNA-microarray and miRNA-microarray

DNA-microarray assays and data analysis have been described before (Vetter *et al.*, 2009). For miRNA-microarray experiments, total RNA was obtained from three independent MCF7-SNAI1 cells induction time course assays as described in (Vetter *et al.*, 2009). Total RNA samples were submitted to the LC Sciences company. Experimental conditions and miRNA-microarray data analyzes were realized by the company as described on their website (www.lcsociences.com).

Luciferase assay

The 3'UTRs of Nectin-1 and StarD10 mRNAs were fused to the renilla gene using the *Xho* I/*Not* I restriction sites of the psiCHECK2vector (Promega). 5.10^4 of 24 h induced MCF7-SNAI1 cells were cotransfected with 50 ng of the indicated vector and 100 nM of the indicated LNA using Lipofectamine 2000 (Invitrogen). Luciferase assays were performed using the Dual-Luciferase assay (Promega). Normalization of the Renilla expression was performed using the Luciferase gene present on the psiCHECK2vector.

siRNA transfection

MCF7 or T47D cells were seeded at a density of 5×10^4 cells per well in a 6-well plate 1 day prior to transfection. Cells were transfected with a specific siRNA of Nectin-1 and/or StarD10 or a control siRNA using Lipofectamine 2000 (Invitrogen) according to the manufacturer's protocol. siRNAs sequences are detailed in Supplemental method1.

Expression of Nectin-1 and StarD10 in tumor patients

Expression profiling of 295 human breast tumors which were previously classified and characterized (Fan *et al.*, 2006; van de Vijver *et al.*, 2002) was analysed using an ANOVA test to statistically evaluate the association between the expression of Nectin-1 and StarD10 with tumor subtype classes.

Acknowledgements:

We wish thanking M. Yatskou and A. Muller (CRP-Santé, Luxembourg) for their help with the microarray data analysis. We are also grateful to C. Hoffmann-Laporte (CRP-Santé, Luxembourg) for her help with confocal microscopy observations. We thank E. Schaffner-Reckinger for critical reading of the manuscript and P. Savagner for helpful discussion about the manuscript.

This work was supported by grants from the Fond National de la Recherche (FNR) du Luxembourg, (BIOSAN), the Fondation Luxembourgeoise Contre le Cancer, Human Frontier Science Program (RGP0058/2005), INSERM and CNRS, France. A. Saumet is a recipient of a fellowship from the Ministere de la Culture, de l'Enseignement Superieur et de la Recherche, Luxembourg (BFR 08/046). M. Moes and A. Le Béhec are supported by AFR grants from the Fond National de la Recherche, Luxembourg.

Footnotes:

Conflict of interest: The authors have no conflicting scientific or financial interest.

References:

- Baek D, Villen J, Shin C, Camargo FD, Gygi SP, Bartel DP. 2008; The impact of microRNAs on protein output . *Nature* . 455 : 64 - 71
- Batlle E, Sancho E, Franci C, Dominguez D, Monfar M, Baulida J . 2000 ; The transcription factor snail is a repressor of E-cadherin gene expression in epithelial tumour cells . *Nat Cell Biol* . 2 : 84 - 9
- Brakeman PR , Liu KD , Shimizu K , Takai Y , Mostov KE . 2009 ; Nectin proteins are expressed at early stages of nephrogenesis and play a role in renal epithelial cell morphogenesis . *Am J Physiol Renal Physiol* . 296 : F564 - 74
- Cano A , Nieto MA . 2008 ; Non-coding RNAs take centre stage in epithelial-to-mesenchymal transition . *Trends Cell Biol* . 18 : 357 - 9
- Cano A , Perez-Moreno MA , Rodrigo I , Locascio A , Blanco MJ , del Barrio MG . 2000 ; The transcription factor snail controls epithelial-mesenchymal transitions by repressing E-cadherin expression . *Nat Cell Biol* . 2 : 76 - 83
- De Craene B , Gilbert B , Stove C , Bruyneel E , van Roy F , Bex G . 2005 ; The transcription factor snail induces tumor cell invasion through modulation of the epithelial cell differentiation program . *Cancer Res* . 65 : 6237 - 44
- De Wever O , Pauwels P , De Craene B , Sabbah M , Emami S , Redeuilh G . 2008 ; Molecular and pathological signatures of epithelial-mesenchymal transitions at the cancer invasion front . *Histochem Cell Biol* . 130 : 481 - 94
- Fan C , Oh DS , Wessels L , Weigelt B , Nuyten DS , Nobel AB . 2006 ; Concordance among gene-expression-based predictors for breast cancer . *N Engl J Med* . 355 : 560 - 9
- Gebeshuber CA , Zatloukal K , Martinez J . 2009 ; miR-29a suppresses tristetraprolin, which is a regulator of epithelial polarity and metastasis . *EMBO Rep* . 10 : 400 - 5
- Gregory PA , Bert AG , Paterson EL , Barry SC , Tsykin A , Farshid G . 2008a ; The miR-200 family and miR-205 regulate epithelial to mesenchymal transition by targeting ZEB1 and SIP1 . *Nat Cell Biol* . 10 : 593 - 601
- Gregory PA , Bracken CP , Bert AG , Goodall GJ . 2008b ; MicroRNAs as regulators of epithelial-mesenchymal transition . *Cell Cycle* . 7 : 3112 - 8
- Hurteau GJ , Carlson JA , Spivack SD , Brock GJ . 2007 ; Overexpression of the microRNA hsa-miR-200c leads to reduced expression of transcription factor 8 and increased expression of E-cadherin . *Cancer Res* . 67 : 7972 - 6
- Kalluri R , Weinberg RA . 2009 ; The basics of epithelial-mesenchymal transition . *J Clin Invest* . 119 : 1420 - 8
- Kim VN , Han J , Siomi MC . 2009 ; Biogenesis of small RNAs in animals . *Nat Rev Mol Cell Biol* . 10 : 126 - 39
- Kong W , Yang H , He L , Zhao JJ , Coppola D , Dalton WS . 2008 ; MicroRNA-155 is regulated by the transforming growth factor beta/Smad pathway and contributes to epithelial cell plasticity by targeting RhoA . *Mol Cell Biol* . 28 : 6773 - 84
- Korpala M , Lee ES , Hu G , Kang Y . 2008 ; The miR-200 family inhibits epithelial-mesenchymal transition and cancer cell migration by direct targeting of E-cadherin transcriptional repressors ZEB1 and ZEB2 . *J Biol Chem* . 283 : 14910 - 4
- Lacroix M . 2006 ; Significance, detection and markers of disseminated breast cancer cells . *Endocr Relat Cancer* . 13 : 1033 - 67
- Lecellier CH , Dunoyer P , Arar K , Lehmann-Che J , Eyquem S , Himber C . 2005 ; A cellular microRNA mediates antiviral defense in human cells . *Science* . 308 : 557 - 60
- Ma L , Young J , Prabhala H , Pan E , Mestdagh P , Muth D . miR-9, a MYC/MYCN-activated microRNA, regulates E-cadherin and cancer metastasis . *Nat Cell Biol* . 12 : 247 - 56
- Murphy NC , Biankin AV , Millar EK , McNeil CM , O'Toole SA , Segara D . 2009 ; Loss of STARD10 expression identifies a group of poor prognosis breast cancers independent of HER2/Neu and triple negative status . *Int J Cancer* .
- Olayioye MA , Hoffmann P , Pomorski T , Armes J , Simpson RJ , Kemp BE . 2004 ; The phosphoprotein StarD10 is overexpressed in breast cancer and cooperates with ErbB receptors in cellular transformation . *Cancer Res* . 64 : 3538 - 44
- Olayioye MA , Vehring S , Muller P , Herrmann A , Schiller J , Thiele C . 2005 ; StarD10, a START domain protein overexpressed in breast cancer, functions as a phospholipid transfer protein . *J Biol Chem* . 280 : 27436 - 42
- Onder TT , Gupta PB , Mani SA , Yang J , Lander ES , Weinberg RA . 2008 ; Loss of E-cadherin promotes metastasis via multiple downstream transcriptional pathways . *Cancer Res* . 68 : 3645 - 54
- Park SM , Gaur AB , Lengyel E , Peter ME . 2008 ; The miR-200 family determines the epithelial phenotype of cancer cells by targeting the E-cadherin repressors ZEB1 and ZEB2 . *Genes Dev* . 22 : 894 - 907
- Peinado H , Olmeda D , Cano A . 2007 ; Snail, Zeb and bHLH factors in tumour progression: an alliance against the epithelial phenotype? . *Nat Rev Cancer* . 7 : 415 - 28
- Reddy SD , Pakala SB , Ohshiro K , Rayala SK , Kumar R . 2009 ; MicroRNA-661, a c/EBPalpha target, inhibits metastatic tumor antigen 1 and regulates its functions . *Cancer Res* . 69 : 5639 - 42
- Sabbah M , Emami S , Redeuilh G , Julien S , Prevost G , Zimmer A . 2008 ; Molecular signature and therapeutic perspective of the epithelial-to-mesenchymal transitions in epithelial cancers . *Drug Resist Updat* . 11 : 123 - 51
- Sakisaka T , Ikeda W , Ogita H , Fujita N , Takai Y . 2007 ; The roles of nectins in cell adhesions: cooperation with other cell adhesion molecules and growth factor receptors . *Curr Opin Cell Biol* . 19 : 593 - 602
- Sarrio D , Rodriguez-Pinilla SM , Hardisson D , Cano A , Moreno-Bueno G , Palacios J . 2008 ; Epithelial-mesenchymal transition in breast cancer relates to the basal-like phenotype . *Cancer Res* . 68 : 989 - 97
- Saumet A , Vetter G , Bouttier M , Portales-Casamar E , Wasserman WW , Maurin T . 2009 ; Transcriptional repression of microRNA genes by PML-RARA increases expression of key cancer proteins in acute promyelocytic leukemia . *Blood* . 113 : 412 - 21
- Takai Y , Miyoshi J , Ikeda W , Ogita H . 2008 ; Nectins and nectin-like molecules: roles in contact inhibition of cell movement and proliferation . *Nat Rev Mol Cell Biol* . 9 : 603 - 15
- Thiery JP , Sleeman JP . 2006 ; Complex networks orchestrate epithelial-mesenchymal transitions . *Nat Rev Mol Cell Biol* . 7 : 131 - 42
- van de Vijver MJ , He YD , van't Veer LJ , Dai H , Hart AA , Voskuil DW . 2002 ; A gene-expression signature as a predictor of survival in breast cancer . *N Engl J Med* . 347 : 1999 - 2009
- Vetter G , Le Béhec A , Muller J , Muller A , Moes M , Yatskou M . 2009 ; Time-resolved analysis of transcriptional events during SNAI1-triggered epithelial to mesenchymal transition . *Biochem Biophys Res Commun* . 385 : 485 - 91

Figure 1

Time resolved transcriptomic analysis of early miRNAs during EMT in inducible MCF7 cells expressing SNAI1

(A), Immunofluorescence and DAPI staining realized with Texas Red phalloidin, specific anti-Cytokeratin-18 (KRT18) and anti-E-Cadherin antibodies in non-induced and 48 h induced MCF7-SNAI1 cells. White bar, 20 μ m. SNAI1 induction in MCF7-SNAI1 cells was obtained by removing Tetracycline from the culture media (represented in figures by -Tet), conversely the presence of tetracycline repressed SNAI1 expression (represented in figures by +Tet). (B) (C), Evaluation of the MCF7-SNAI1 cell motility after 24 h SNAI1 induction using uncoated Transwells for cell migration (B) or Matrigel-coated Transwells for cell invasion (C). (D), Detection of expression of miR-200a, miR-200b and miR-429 by miRNA-microarrays in MCF7-SNAI1 cells at different time points after SNAI1 induction. (E), Evaluation of the number of mRNAs predicted to be targeted by each miRNA found to be up-regulated at a time point preceding 12 h after SNAI1 induction. mRNAs that were found previously to be up-or down-regulated after SNAI1 induction (Vetter *et al.* , 2009) were selected for this analysis. miRbase software (version 13) was used for the target prediction using a minimal score of 17. NA, means prediction Non Available. (F), Quantitative Real-time PCR analyses of miR-661 expression realized in MCF7-SNAI1 cells at different time points after SNAI1 induction. Results are represented as the mean \pm s.e.m (standard error of mean) of at least 3 independent experiments.

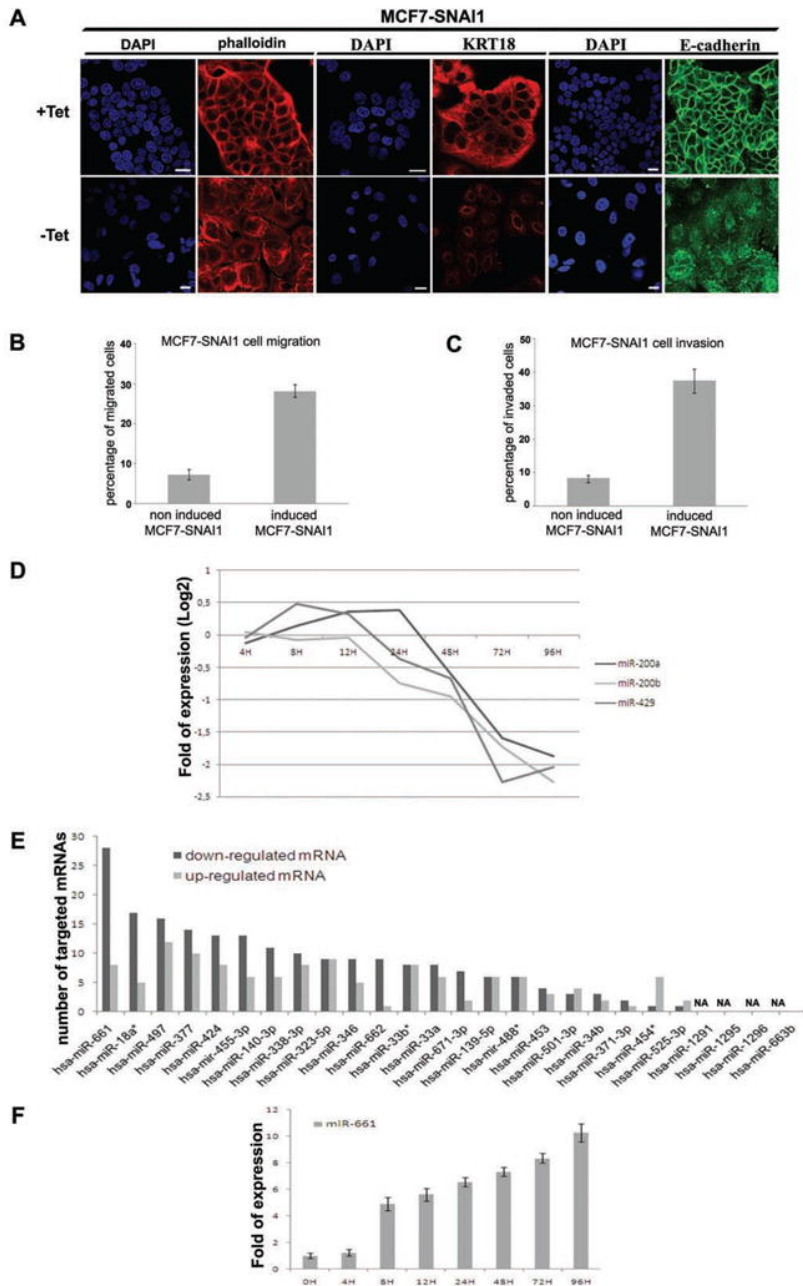


Figure 2

Expression of miR-661 is required for cell invasion and migration of invasive breast cancer cell lines

(A), Transwell migration assay and Matrigel invasion assay (bottom) of MCF7-SNAI1 induced cells transfected with the miR-661-specific antisens LNA (LNA-661), or with the scrambled LNA (LNA-sc). (B), Real-time PCR analysis of the expression of epithelial markers (cytokeratin-18 (KRT18), E-cadherin, Claudin-3 and beta-catenin) in non-induced or induced-MCF7-SNAI1 cells, transfected with miR-661-specific antisense LNA (LNA-661), or with scrambled LNA (LNA-sc). (C), Real-time PCR analysis of miR-661 expression in six different cell lines. (D), Transwell migration assay and Matrigel invasion assay (bottom) of MDA-435 transfected with LNA-661 or with LNA-sc. Cell migration and invasion was analyzed 24 h after the seeding in the transwells. Results are represented as the mean \pm s.e.m (standard error of mean) of at least 3 independent experiments.

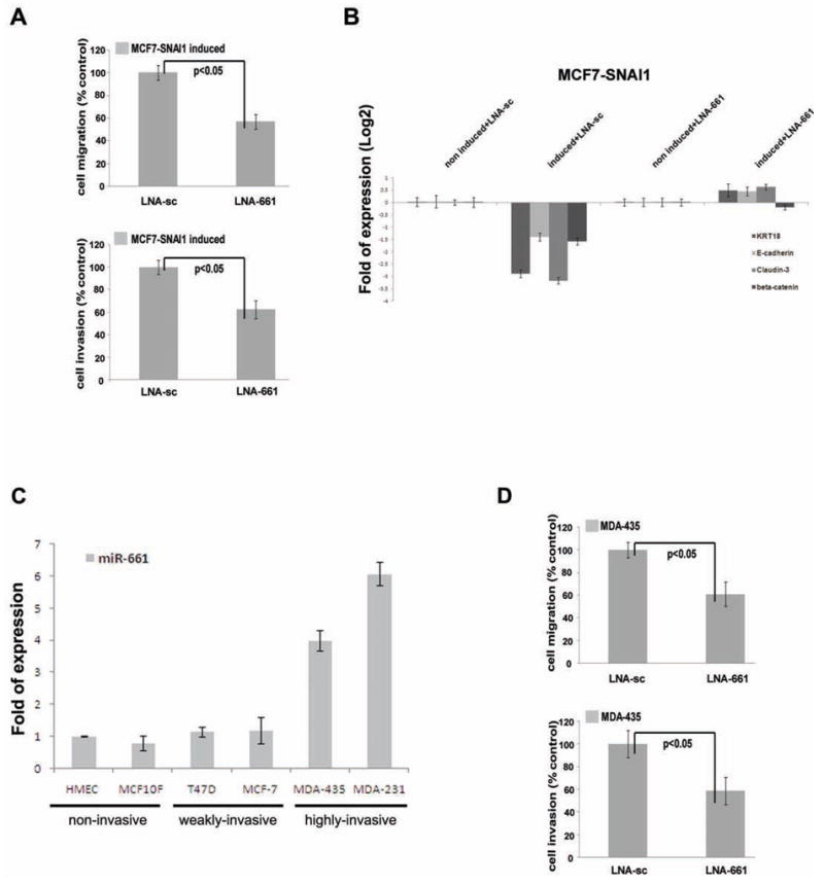


Figure 3

miR-661 regulates the expression of Nectin-1 and StarD10

(A), Representative selection of predicted candidates mRNA 3'UTR target binding sites of miR-661. Predictions were performed using miRBase Target release 13 (<http://microrna.sanger.ac.uk>). (B), (C), Evaluation of the mRNA expression level by real-time PCR (B), and of the protein level by immunoblot analysis (C), 48 h after forced ectopic expression of pSuper-miR-661 vector or pSuper-empty vector as a negative control in MCF7-SNAI1 cells. (D), Monitoring by real-time PCR of Nectin-1 and StarD10 (bottom) expression after SNAI1 induction in MCF7-SNAI1 cells. Results are represented as the mean \pm s.e.m (standard error of mean) of at least 3 independent experiments.

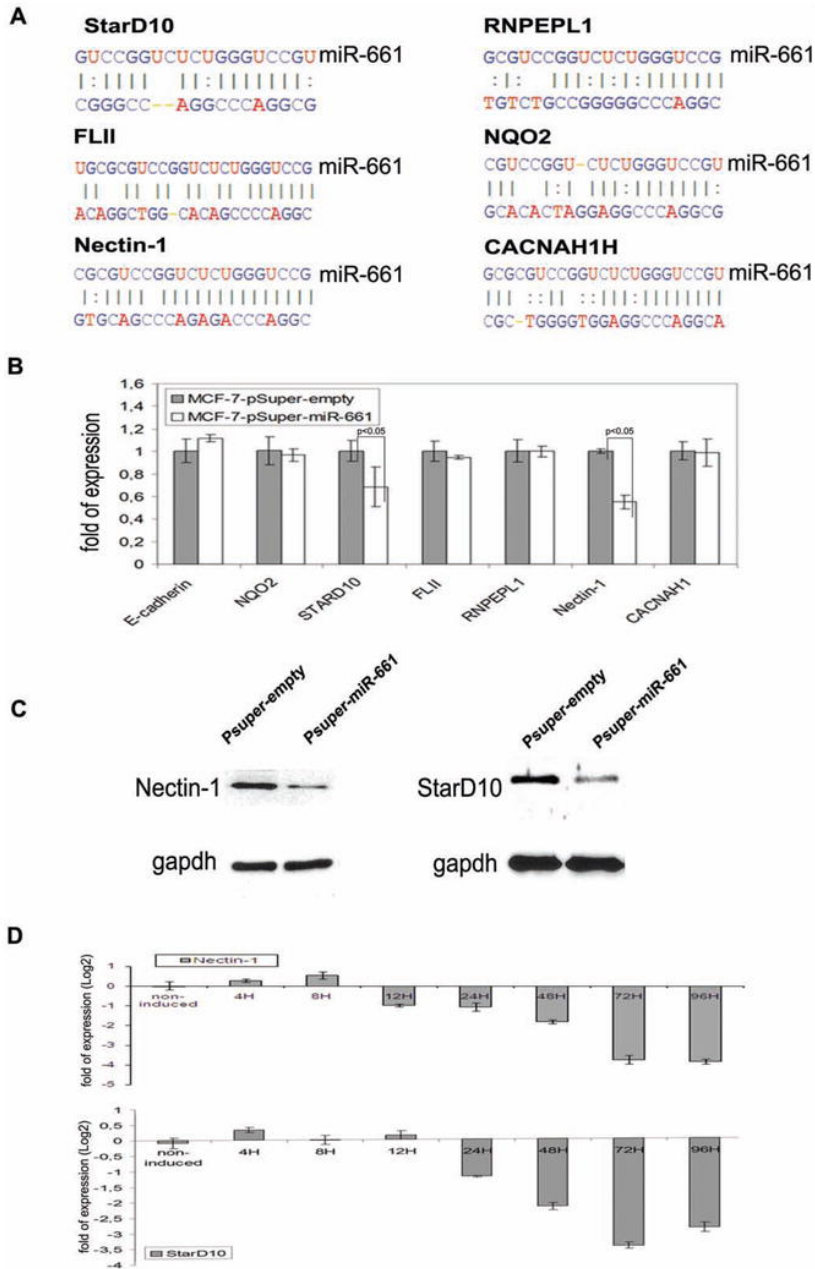


Figure 4

Subcellular localization of Nectin-1 and StarD10 in MCF7-SNAI1 cells upon induction of SNAI1

(A), Immunofluorescence and phalloidin staining realized with specific anti-Nectin-1 and anti-E-Cadherin antibodies in non-induced (+Tet) MCF7-SNAI1 cells. (B), (C), Immunofluorescence and DAPI staining realized with StarD10-, E-Cadherin- (B) or ZO-1-specific (C) antibodies in non-induced (+Tet) MCF7-SNAI1 cells. (D), (E) Immunofluorescence and DAPI staining were realized in non-induced (+Tet) and induced (- Tet, 48 h after induction) MCF7-SNAI1 cells using specific anti-SNAI1 (D,E), anti-Nectin-1 (D) or anti-Stard10 (E) antibodies. Bars, 10 μ m.

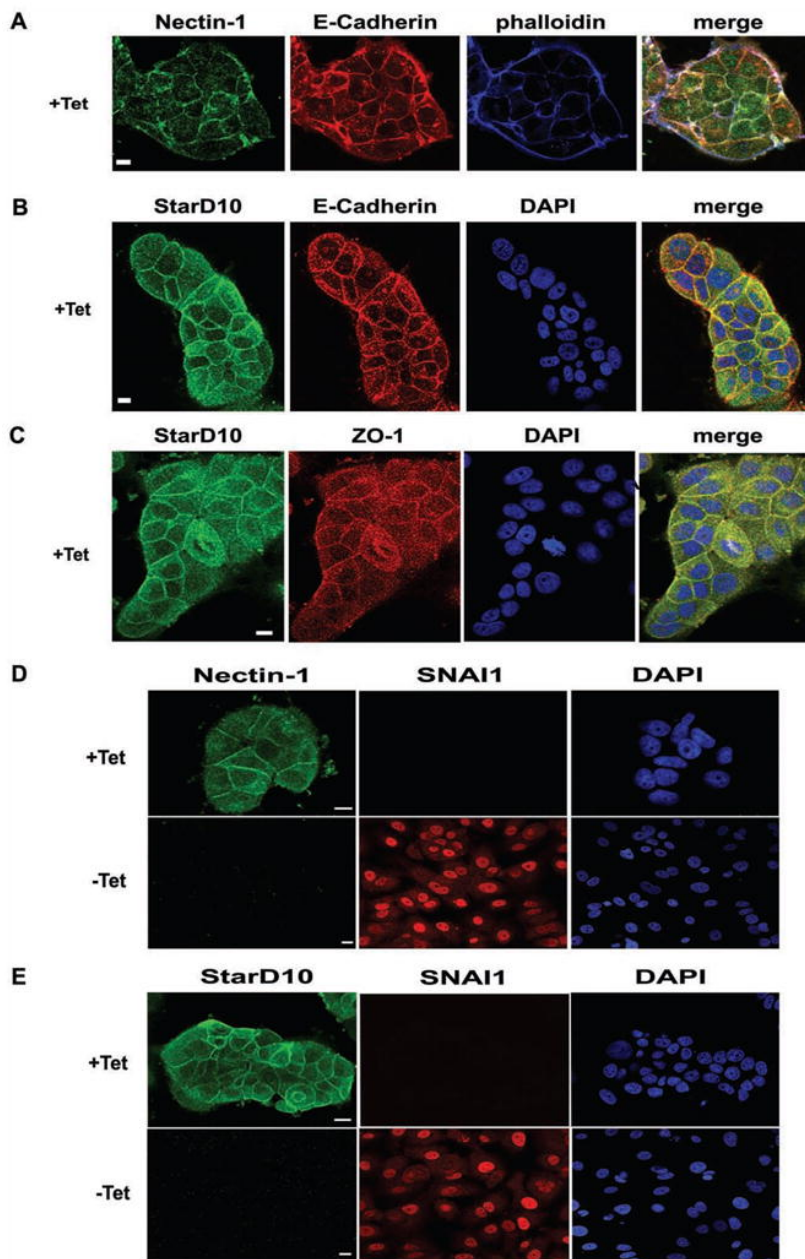


Figure 5

3'-UTR of Nectin-1 and Stard10 messengers are sensitive to miR-661

(A), (B), Evaluation of miR-661 candidate target gene expression by real-time PCR (A), and immunoblot analysis (B), in induced (-Tet) or non-induced (+Tet) MCF7-SNAI1 cells transfected with LNA-661 or LNA-sc. Protein and mRNA levels were analyzed 48 h after SNAI1 induction. Immunoblot assays were realized with specific antibodies against StarD10, Nectin-1 or gapdh, as a control. (C), Evaluation of the sensitivity of the 3'UTRs of Nectin-1 and StarD10 mRNAs to miR-661. Luciferase assay were performed with 48 h induced MCF7-SNAI1 cells. Cells were transfected with the empty *renilla* luciferase reporter gene (psiCHECK2) or the reporter gene fused to the Nectin-1 or StarD10 3'UTR (psiCHECK2-3'UTRnectin-1, psiCHECK2-3'UTRStarD10). In addition, the cells were cotransfected or not with the LNA-sc or LNA-661. Results are expressed as Relative Light Units (RLU) and were normalized with the luciferase activity expressed constitutively by the psiCHECK2 vector. Results are represented as the mean +/- s.e.m (standard error of mean) of at least 3 independent experiments.

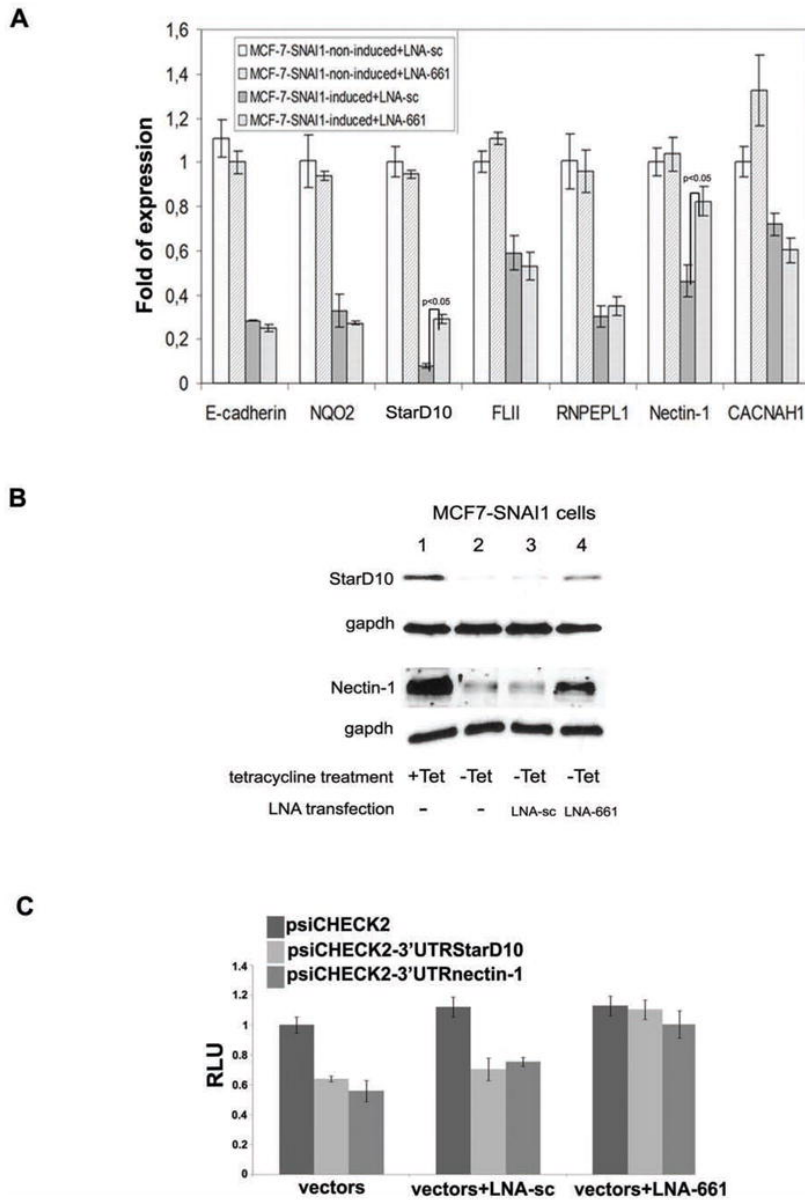


Figure 6

Evaluation of Nectin-1 and StarD10 expression in breast cancer cell lines and their impact on EMT-induced cell invasion in induced MCF7-SNAI1 cells

(A), (B), Real-time PCR analysis of Nectin-1 (A) and StarD10 (B) expression in breast cancer cell lines. (C), Real-time PCR analysis of Nectin-1, StarD10 and epithelial markers expression (cytokeratin-18 (KRT18), E-cadherin, Claudin-3 and beta-catenin) in MCF7 (left) or T47D (right) cells transfected with the siRNA of the Nectin-1 (SiRNA-Nectin-1), StarD10 (SiRNA-StarD10), both (SiRNA-Nectin-1/SiRNA-StarD10) or with control siRNA (SiRNA-neg). (D), Transwell Matrigel invasion assay of induced MCF7-SNAI1 cells transfected with GFP-Nectin-1, GFP-StarD10 or GFP, as a control. Invasion assays were realized 24 h after MCF7-SNAI1 cell induction and transfection with the vectors. Experiments were realized in three independent triplicates. Error bars indicate s.e.m.

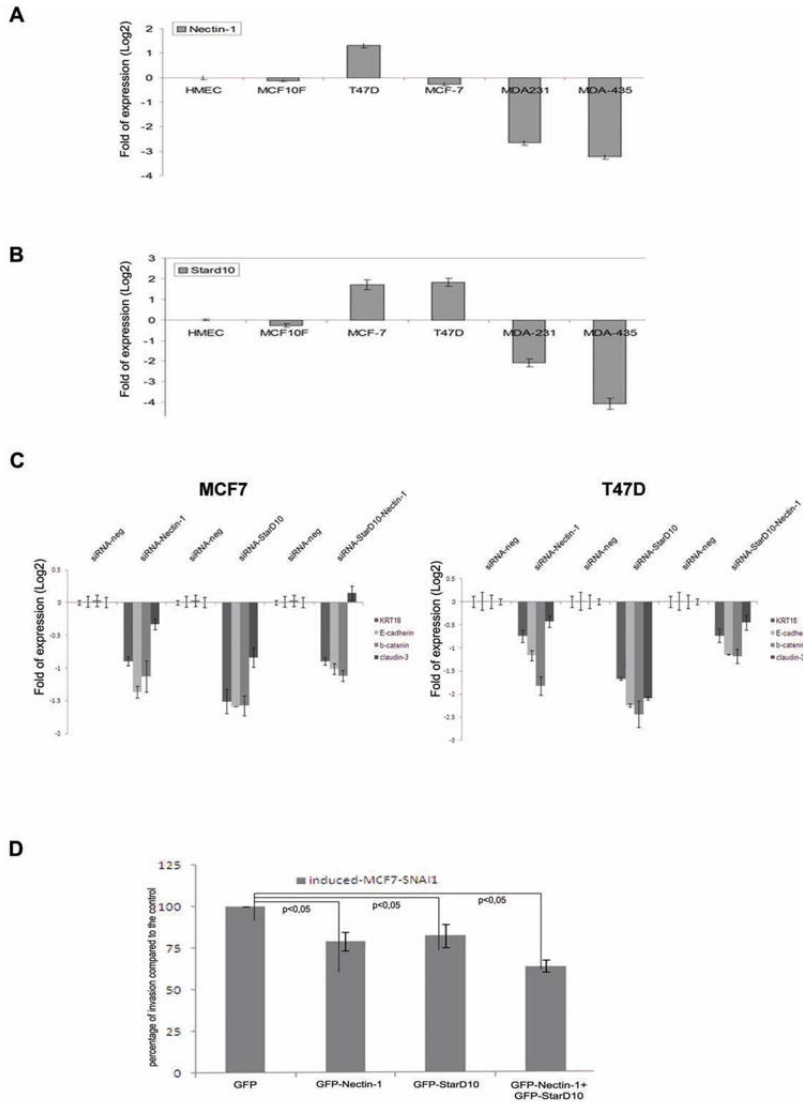


Figure 7

Evaluation of StarD10 expression in human breast tumors

Expression of StarD10 in basal-like (BL), Luminal A, B (LA and LB), normal-like breast (NBL) and Her2+ (HR) breast tumors subtypes of 295 human breast tumors characterized in a previous study (van de Vijver *et al.*, 2002).

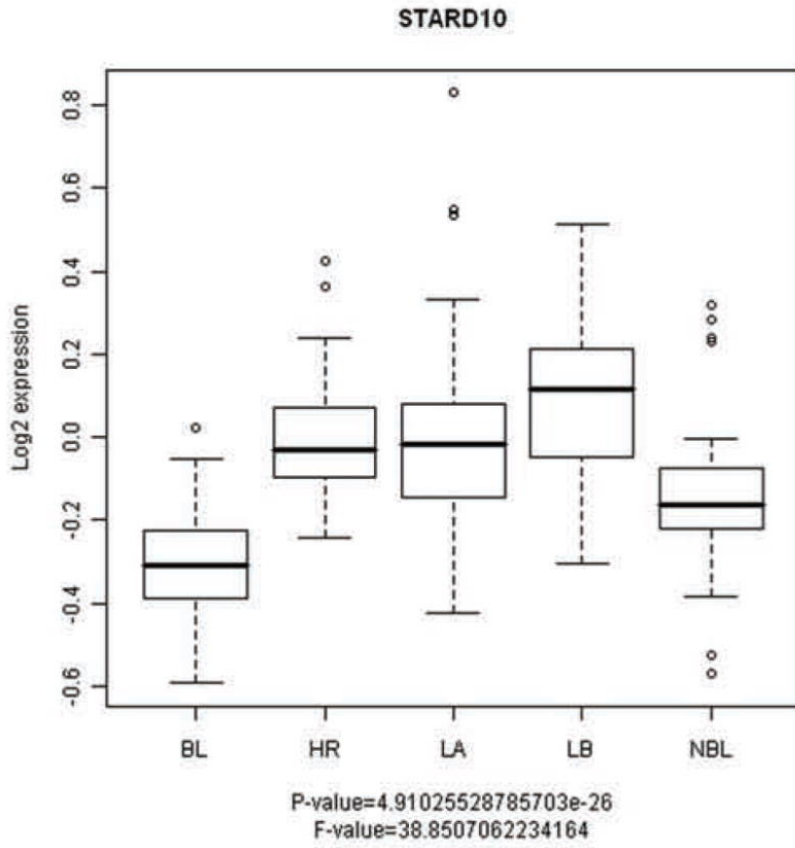


Table 1

Pearson correlation analysis between StarD10 and tumor markers expression

Pearson correlation association between StarD10 and tumor markers genes expression in the 295 breast tumors characterized by (van de Vijver *et al.* , 2002).

	StarD10
Basal-Like markers	
<i>KRT5</i>	-0,31702
<i>KRT14</i>	-0,14909
<i>FOXC1</i>	-0,51169
Luminal markers	
<i>FOXA1</i>	0,552127
<i>GATA3</i>	0,501762
<i>KRT18</i>	0,57425
<i>KRT8</i>	0,495991